

An Adaptive Fast Multipole Approach to 2D Wave Propagation

V. Mallardo¹ and M.H. Aliabadi²

Abstract: The present paper intends to couple the Fast Multipole Method (FMM) with the Boundary Element Method (BEM) in the 2D scalar wave propagation. The procedure is aimed at speeding the computation of the integrals involved in the governing Boundary Integral Equations (BIEs) on the basis of the distance between source point and integration element. There are three main contributions. First, the approach is of adaptive type in order to reduce the number of floating-point operations. Second, most integrals are evaluated analytically: the diagonal and off-diagonal terms of the H and G matrices by consolidated techniques, whereas the moment M_k by a procedure developed by the authors. Third, the article is enriched by Fortran 90 schemes that, specifically developed by the authors, allow the optimum construction of the quad-tree and of the iterative system of equations. The Generalized Minimal Residual Solver is adopted to improve the overall computational efficiency. Some numerical examples are shown to demonstrate the reliability of the method.

Keywords: Fast multipole method, Boundary Element Method, Helmholtz equation.

1 Introduction

The BEM has been used to solve interior/exterior acoustic problems for many years because of its boundary only discretisation and automatic satisfaction of the radiation condition at infinity (see for instance Wrobel 2002 for linear acoustics and Mallardo and Aliabadi 2011 for nonlinear acoustics). The main drawback is related to the final system of equations which results to have dense, non-symmetrical and sometimes ill-conditioned coefficient matrices. Solving the system of equations

¹ Corresponding author. mlv@unife.it. Dep. Architecture, University of Ferrara, Via Quartieri 8 44121 Ferrara, Italy

² m.h.aliabadi@imperial.ac.uk. Dep. Aeronautics, Imperial College London, South Kensington Campus, UK

becomes prohibitively expensive when applied to large-scale engineering problems. In fact, the computation of the coefficients of the matrices governing the discrete problem requires $O(N^2)$ operations and another $O(N^3)$ operations is necessary to solve the system using any direct solver (let N be the number of equations).

In 1983 Rokhlin proposed an algorithm for rapid solution of classical boundary value problems for the Laplace equation based on iteratively solving integral equations of potential theory. The CPU time requirement obtained was proportional to N . The starting point was the harmonic expansion of the kernel. The algorithm appeared to be the most efficient of the at that time available tools for the solution of large scale boundary value problems whenever the solution needed to be evaluated at a limited number of points. The procedure was then extended, a few years later, to two dimensional acoustic scattering in Rokhlin (1990) where the author described a similar procedure capable to reduce the CPU time requirements of the algorithm to $N^{4/3}$. In both papers no connection with the BEM was introduced.

It took almost ten years for scientific community to realise the potential capability of coupling the FMM with the BEM. A comprehensive review of the fundamentals of FMM and FMM accelerated Boundary Integral Equation Method (BIEM) with reference to the Laplace and Helmholtz equations is surveyed in Nishimura (2000). With conventional BIEM it is not possible to solve beyond several thousands of unknowns with a desktop computer. Actually, methods of solution of problems of the size of more than 10^8 unknowns (which roughly correspond to 10^6 unknowns in the BEM context) are investigated in FEM with massively parallel computers. With fast multipole accelerated BIEM, problems of the size of 10^6 unknowns can be handled even in desktop computers. However, the use of the FMM has increased the complexity in implementations of the BEM: the structure of the code changes completely and the pre-processor stage becomes more important than in the conventional approach. An interesting introduction to the Fast Multipole Boundary Element Method (FMBEM) for potential problems is presented in Liu and Nishimura (2006): the structure of a FMBEM program along with the details of the method with reference to the Laplace equation are presented.

An application of the FMM to the Dual Boundary Element Method (DBEM) for the analysis of finite solids with large numbers of microcracks is given in Wang, Yao and Lei (2006).

An adaptive FMBEM for 3D acoustic wave problems is investigated in Shen and Liu (2007) where the Burton-Miller formulation is applied to overcome the non-uniqueness difficulties. The adaptive approach is demonstrated to be several times faster than the non-adaptive FMBEM while maintaining the accuracy of the BEM. The procedure illustrated in Chen and Chen 2004 represents an application of the

FMBEM to 2D acoustic problems. The FMM is used to accelerate the construction of the influence matrix in the BEM. The approach is of non-adaptive type and the number of floating-point operations is reduced from $O(N^2)$ to $O(N \log^a N)$ where a is a small constant independent on N . Further improvement is reached in Li and Huang (2011) where the BEM is fully coupled to the FMM in large-scale two dimensional acoustic problems based on the improved Burton-Miller formulation. A new definition of the interaction list is introduced in Bapat and Liu (2010) in order to reduce the computational effort to execute the moment-to-local translations.

Adaptive cross approximation (ACA) and hierarchical matrix format represent an alternative to FMM in dealing with large-scale problems with similar performance. Examples of application of such techniques in the acoustic field are given in Mallardo et al. (2011) and in Brancati, Aliabadi and Mallardo (2012) whereas comparison of the FMM with Hierarchical Matrices for the Helmholtz equation is given in Brunner et al. (2010).

This paper intends to present a FMBEM for two-dimensional scalar wave propagation, i.e. fields governed by the Helmholtz equation. In spite 2D models are, in principle, less power than 3D ones, the 2D approach may result very useful in many large-scale applications in which the repetitive character of the geometry and of the loads allows the use of 2D models, and hence the investigation, with higher and higher frequencies in reasonable CPU time. The 2D approach is attractive, for instance, in optimisation and identification problems as well as in passive noise control, i.e. where either the solution is to be obtained iteratively many times or the frequency under investigation is particularly high.

An iterative Generalized Minimal Residual Solver (GMRES) is adopted to improve the overall computational efficiency. There are three main novelties in the paper: 1) the multipole approach is of adaptive type; 2) most of the integral terms are evaluated analytically, the moment M_k by a procedure specifically developed and tested by the authors; 3) finally, the construction of the quad-tree and of the final system of equations is achieved in the Fortran 90 context, thus allowing the minimization of both the CPU-time effort and the hard-disk capabilities. After this Introduction, the integral equations which govern the 2D acoustic problem are presented along with the main relations of the FMM in Section 2. Afterward, in Section 3, the algorithm and the integration schemes are detailed. All the integrals evaluated analytically are detailed in Section 4. Finally, in Section 5, some numerical examples are investigated in order to measure the reliability of the procedure when compared to an analytical solution and to test it for multiple scattering in the high frequency range. The paper is enriched with one Appendix detailing the analytical solutions which were useful to check the numerical results.

2 The FMBEM relations

The propagation of time-harmonic acoustic waves in a homogeneous isotropic acoustic medium (either finite or infinite) is described by the Helmholtz equation:

$$\nabla^2 p(\mathbf{x}) + k^2 p(\mathbf{x}) = 0 \quad (1)$$

under the boundary conditions:

$$p(\mathbf{x}) = \bar{p}(\mathbf{x}) \quad \mathbf{x} \in \Gamma_1 \quad (2a)$$

$$q(\mathbf{x}) = p(\mathbf{x})_{,n} = \bar{q}(\mathbf{x}) \quad \mathbf{x} \in \Gamma_2 \quad (2b)$$

where p is the acoustic pressure, $k = \omega/c$ with ω = angular frequency and c = sound velocity, comma indicates partial derivative, $\Gamma_1 \cup \Gamma_2 = \Gamma$, Γ is the boundary of the domain Ω under analysis, $\mathbf{n} = \mathbf{n}(\mathbf{x})$ is the outward normal to the boundary in \mathbf{x} , q is the flux and the barred quantities indicate given values.

The boundary value problem described by the above equations can be transformed into the following integral representation (Wrobel 2002, Aliabadi 2002):

$$c(\boldsymbol{\xi})p(\boldsymbol{\xi}) + \int_{\Gamma} q^*(\boldsymbol{\xi}, \mathbf{x})p(\mathbf{x})d\Gamma(\mathbf{x}) - \int_{\Gamma} p^*(\boldsymbol{\xi}, \mathbf{x})q(\mathbf{x})d\Gamma(\mathbf{x}) = 0 \quad (3)$$

where $c(\boldsymbol{\xi})$ occurs in the limiting process from the internal point to the boundary point, being equal to 0.5 if the tangent line to the boundary at $\boldsymbol{\xi}$ is continuous. The fundamental solutions p^* and q^* are given by:

$$p^*(\boldsymbol{\xi}, \mathbf{x}) = \frac{i}{4}H_0^{(1)}(kr) \quad (4a)$$

$$q^*(\boldsymbol{\xi}, \mathbf{x}) = -\frac{ik}{4}H_1^{(1)}(kr)r_{,n} \quad (4b)$$

where $H_0^{(1)}$ and $H_1^{(1)}$ are the Hankel function of the first kind, 0th and 1st order respectively, $r = \|\mathbf{x} - \boldsymbol{\xi}\|$ is the distance between the collocation point $\boldsymbol{\xi}$ and the field point \mathbf{x} .

The conventional BEM numerical procedure is based on two steps: first, the discretisation of the boundary Γ , second, the collocation of the Eq. (3) in each node in order to build a final (square) system of equations in the unknowns either p or q on the boundary. In the present contribution constant elements are adopted: with such a choice all the integrals involved are performed analytically. The discretised equation collocated at node $\boldsymbol{\xi}_i$ can be written as:

$$c(\boldsymbol{\xi}_i)p(\boldsymbol{\xi}_i) + \sum_{j=1}^n p_j \int_{\Gamma_j} q^*(\boldsymbol{\xi}_i, \mathbf{x})d\Gamma(\mathbf{x}) = \sum_{j=1}^n q_j \int_{\Gamma_j} p^*(\boldsymbol{\xi}_i, \mathbf{x})d\Gamma(\mathbf{x}) \quad (5)$$

In the conventional approach, the source node ξ_i is collocated at each node in order to build a linear system of equations of this type:

$$\mathbf{H}\mathbf{p} = \mathbf{G}\mathbf{q} \quad (6)$$

where matrices \mathbf{H} and \mathbf{G} collect integrals of the fundamental solutions, whereas \mathbf{p} and \mathbf{q} are vector collecting pressure and flux on the boundary. After imposing the boundary conditions (2), the above system of equations can be re-written in the conventional way:

$$\mathbf{A}\mathbf{x} = \mathbf{b} \quad (7)$$

where the matrix \mathbf{A} is obtained by suitably interchanging columns of \mathbf{H} and \mathbf{G} in accordance with the given boundary conditions.

If an iterative solver is adopted, the product on the left hand side of (7) is to be evaluated iteratively many times till the solution is obtained. Therefore, the procedure requires the evaluation of either the integral of p^* or the integral of q^* on each boundary element. Each integral can be obtained in a much faster way by adopting the Fast Multipole approach detailed below.

For convenience, the complex notation is introduced, i.e. the collocation and field points are replaced by their complex representation:

$$\xi = z_0 = \xi_1 + i\xi_2 \quad (8a)$$

$$\mathbf{x} = z = x_1 + ix_2 \quad (8b)$$

with $i = \sqrt{-1}$. With such an assumption it is simple to show that the fundamental solutions in ξ, \mathbf{x} coincide with their expression in complex notation:

$$p^*(\xi, \mathbf{x}) = p^*(z_0, z) \quad (9a)$$

$$q^*(\xi, \mathbf{x}) = q^*(z_0, z) \quad (9b)$$

The FMM relations intervene on the evaluation of the integrals involved in the Eq. (5). The multipole expansion is the key point in reducing the CPU time which is necessary to evaluate each integral. If $F(z_0, z)f$ indicates either $p^*(z_0, z)q$ or $q^*(z_0, z)p$, the following *local expansion* can be obtained:

$$\int_{\Gamma_j} F(z_0, z) f d\Gamma(z) = \frac{i}{4} \sum_{p=-\infty}^{\infty} (-1)^p L_{-p}(z_L) I_p(z_0 - z_L) \quad (10)$$

where:

$$I_p(z) = (-i)^p J_p(kr) e^{ip\theta} \quad (11)$$

r, θ are the polar coordinates of z and J_p stands for the Bessel function of the p^{th} order.

The coefficients L_{-p} are given by the following *M2L translation*:

$$L_l(z_L) = \sum_{k=-\infty}^{\infty} O_{k+l}(z_L - z_C) P_{-k}(z_C) \quad (12)$$

where $\|z_0 - z_L\| < \|z_C - z_L\|$ must be satisfied and:

$$O_m(z) = i^m H_m^{(1)}(kr) e^{im\theta} \quad (13)$$

The term $P_k(z_C)$ is called *moment about z_C* , it is independent of the collocation point z_0 and it only needs to be computed once. The expression of M_k and N_k is given as follows:

$$M_k(z_C) = q \int_{\Gamma_j} I_k(z - z_C) d\Gamma(z) \quad (14a)$$

$$N_k(z_C) = p \int_{\Gamma_j} \frac{\partial I_k(z - z_C)}{\partial \mathbf{n}} d\Gamma(z) \quad (14b)$$

The point z_C is assumed to be located close to Γ_j so that

$$\max_{z \in \Gamma_i} \|z - z_C\| < \|z_0 - z_C\| \text{ holds.}$$

The series expansion (12) involving P_k can be truncated to *nexp* terms with a good approximation if *nexp* is set larger than kr_{max} (see Rokhlin, 1990 for details).

If the point z_C is moved to a new location $z_{C'}$, the following *M2M translation* is obtained:

$$P_p(z_{C'}) = \sum_{m=-\infty}^{\infty} I_{p-m}(z_C - z_{C'}) P_m(z_C) \quad (15)$$

Analogously, if the point for local expansion is moved from z_L to $z_{L'}$, the following *L2L expansion* is obtained:

$$L_l(z_L) = \sum_{k=-\infty}^{\infty} I_{l-k}(z_{L'} - z_L) L_k(z_{L'}) \quad (16)$$

3 The algorithm

The adaptive procedure starts from a square containing the entire boundary and then repeatedly divides it and the successive sub-cells into four sub-squares until a fixed maximum number of boundary elements is contained in each cell. In Fig. 1 the subdivision process up to the last level is depicted with the allowed maximum number of elements set to one. Each of the final cells of the division process (in the figure the cells containing one element) is also called *leaf*.

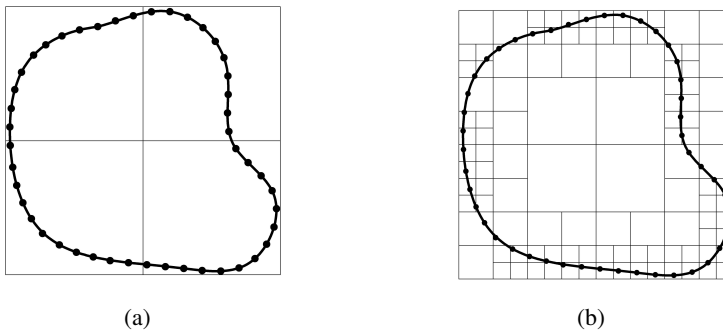


Figure 1: Square division at level 1 (a) and up to level 4 (b)

The construction of the tree, in 2D it can be called quad-tree, is a keypoint in developing an efficient code. In fact, the size of the matrices and the vectors involved is not known in advance but it can be computed only after the complete construction of the quad-tree. In the present paper the capability provided by Fortran 90 language with *type*, *pointer* and *recursive subroutine* is adopted to accomplish such a task. If two new types are defined, i.e.:

TYPE data

....

cell details

....

END TYPE data

TYPE cell

type(data) :: data_cell

type(cell), pointer :: bl,br,tl,tr

END TYPE cell

where *bl,br,tl,tr* point to the four subcells, then, a recursive subroutine can be de-

veloped in order to build recursively the entire quad-tree:

RECURSIVE SUBROUTINE BUILD_TREE(.....,p_cell_i,.....)

....

type(cell), pointer :: p_cell_i

....

associate p_cell_i if not associated

assign the details of the cell

divide the cell if not leaf

call UPDATE_TREE for each sub-cell

END SUBROUTINE BUILD_TREE

For a given collocation node z_0 , the integral over the entire boundary is determined in different way on the basis of the distance $\|z - z_0\|$. If the integration element is *close* (where *close* means either in the same cell or in one of the cells surrounding it, see Fig. 2(a)) to the collocation node, the integral contribution is determined directly as in the conventional BEM. Given the source point in Z_0 , such an integration is performed along the red elements in Fig. (2a) in the analytic way which will be detailed in the successive section. On the other hand, if the position of the integration element with respect to the collocation node is as depicted in red in Fig. 2(b), i.e. the integration element belongs to the cell whose parent is adjacent to the parent of the collocation node's cell, the Eq. (10) is applied via the *M2L translation*. Finally, the contribution from far cells (depicted in Fig. 2c) is obtained by the local expansion via the *L2L translation*.

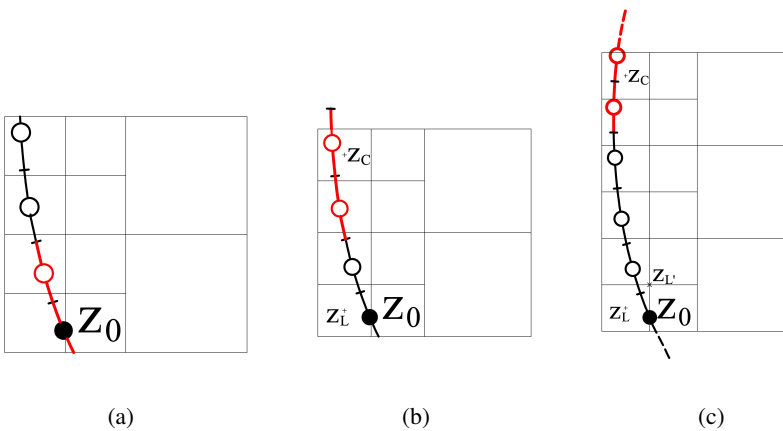


Figure 2: Direct (a), M2L (b) and L2L (c) integrations.

The elements of the matrix A of the final system of equations $\mathbf{Ax} = \mathbf{b}$ are not stored. The product \mathbf{Ax}_i is evaluated iteratively until the solution converges within a given tolerance. The GMRES method is adopted. It was first proposed by Saad and Schultz (1986) in order to solve large, sparse and nonsymmetric linear systems. The routine implemented in the paper stores the banded diagonal of the governing matrix A as preconditioner, i.e. if $nlmax$ indicates the maximum number of elements allowed in a leaf, the preconditioner is a $nlmax$ -banded diagonal matrix collecting the A_{ij} coefficients evaluated analytically when source point and integration element belong to the same cell.

4 The analytical integration

The FMBEM procedure requires the evaluation of some integrals. Some of them are involved in the direct integration whereas two integrals are necessary to evaluate the moments in the Eq. (14).

Diagonal term of the matrix H. The term H_{ii} involving the fundamental solution q^* when the source node belongs to the integration element is zero as constant elements are adopted, i.e. $r_{,n} = 0$.

Diagonal term of the matrix G. The diagonal term G_{ii} can be determined analytically by using the procedure presented in Singh and Tanaka (2000):

$$\int_{\Gamma_{AB}} p^*(\boldsymbol{\xi}, \mathbf{x}) d\Gamma(\mathbf{x}) = \frac{i}{4} l_{AB} \left[H_0^{(1)}\left(k \frac{l_{AB}}{2}\right) + \frac{\pi}{2} \left(\hat{H}_0\left(k \frac{l_{AB}}{2}\right) H_1^{(1)}\left(k \frac{l_{AB}}{2}\right) - \hat{H}_1\left(k \frac{l_{AB}}{2}\right) H_0^{(1)}\left(k \frac{l_{AB}}{2}\right) \right) \right] \quad (17)$$

where $\hat{H}_\nu(z)$ denotes the Struve function of order ν and A and B are the extreme points of the integration element of length l_{AB} . A similar expression can be obtained when the source point does not belong to the integration element but it lies on the line AB .

Off-diagonal terms of the matrices H and G. The H_{ij} and G_{ij} terms (with $i \neq j$) can be analytically evaluated in the case $kr \leq 2$. The case $kr > 2$ can only be solved numerically. As a matter of fact, in the FMBEM context, a boundary discretisation which satisfies 8 – 10 elements for wavelength would never allow kr to be greater than 2, i.e. it would not require a numerical integration. The expression of G_{ij} and

H_{ij} for $kr \leq 2$ are given by:

$$\int_{\Gamma_j} p^*(\boldsymbol{\xi}, \mathbf{x}) d\Gamma(\mathbf{x}) = -\frac{1}{2\pi} \sum_{i=1}^7 \left[\frac{A_i}{2} \bar{P}_{1,i} - B_i P_{2,i} \right] \begin{matrix} \xi_B \\ \xi_A \end{matrix} \quad (18a)$$

$$\int_{\Gamma_j} q^*(\boldsymbol{\xi}, \mathbf{x}) d\Gamma(\mathbf{x}) = \frac{ik}{2\pi} \left[\eta \sum_{i=1}^7 \left(\frac{D_i}{2} P_{1,i} + E_i P_{2,i-1} \right) \right] \begin{matrix} \xi_B \\ \xi_A \end{matrix} \quad (18b)$$

where the terms involved in the above expressions are reported in Ramesh and Lean (1991).

Moments M_k and N_k . The integral expressing the moment N_k is evaluated numerically by Gaussian quadrature, whereas the moment M_k is determined analytically for constant elements. No contributions are available in the scientific literature; the proposed procedure is outlined below.

The keypoint is the determination of the following integral:

$$\int_{\Gamma_{AB}} e^{im\theta} J_m(kr) d\Gamma \quad (19)$$

where m is an integer, $k = \omega/c$ and r, θ are the polar coordinates of the point x, y moving on the segment AB . The integral in Eq. (19) can be expressed in terms of the integral of the Bessel function by the application of the Graf's theorem (see Watson 1966, pag. 360), i.e.:

$$e^{im\psi} J_m(\tilde{\omega}) = \sum_{l=-\infty}^{\infty} J_{m+l}(Z) J_l(z) e^{il\phi} \quad (20)$$

where $Z, z, \psi, \tilde{\omega}$ and ϕ are depicted in Fig. 3.

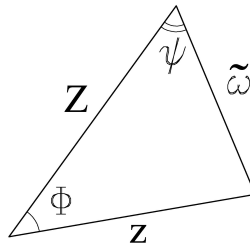


Figure 3: Geometry of the Graf's theorem.

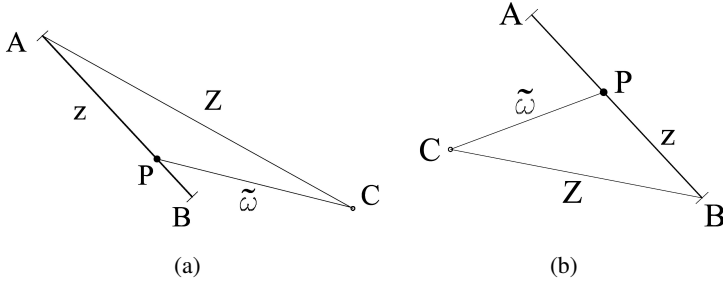


Figure 4: Analytical integration of M_k - The meaning of the symbols involved in the Graf's theorem in two different geometrical situation.

On the basis of the Graf's theorem and of the geometrical representation depicted in Fig. 4, the moment M_k can be expressed in terms of the Bessel integral by the following relation:

$$\int_{\Gamma_{AB}} e^{im\theta} J_m(kr) d\Gamma = \frac{A}{k} \sum_{l=-\infty}^{\infty} J_{l+m}(\bar{Z}) e^{il\bar{\phi}} \int_0^{\bar{z}} J_l(z) dz \quad (21)$$

where $\bar{z} = k|AB|$ and

$$A = \begin{cases} e^{il\theta_{CA}} \\ e^{il\theta_{CB}} \end{cases} \quad \bar{Z} = \begin{cases} k|CA| \\ k|CB| \end{cases} \quad \bar{\phi} = \begin{cases} \widehat{PAC} \\ \widehat{PBC} \end{cases} \quad \begin{matrix} \text{if } \theta_{CA} < \theta_{CP} \\ \text{else} \end{matrix} \quad (22)$$

The origin O of the integration is to be taken coincident either with A or with B provided that $\theta > \theta_{CO}$ (see also Fig. 4).

The integral of the Bessel function:

$$\int_0^T J_\nu(t) dt \quad \forall \nu \geq 0 \quad (23)$$

is given by the expression 11.1.2 for $\nu > 0$ and by the expressions 11.1.11-13 for $\nu = 0$ in Abramowitz and Stegun (1964).

The analytical approach for evaluating the polar moment M_m is compared to the numerical (Gaussian) one in the Tables 1, 2 with reference to the segment AB with $A = (0.,0.)$ and $B = (1.,0.)$ and C , pole of the moment M_m , in two different positions. The results are reported together with the number ng of the Gaussian points and the number $nbes$ of the series expansion terms in Eq. 21 which are necessary to converge to the analytical and numerical results, respectively. From the tables it

is clear that the analytic approach requires a higher number of computations to be performed, on the other hand the numeric integration cannot guarantee to converge to the correct solution in each case. Furthermore, the minimum number of *nbes* can be set of the order of kr where r refers to the distance between C and the segment AB , on the other hand the necessary number of Gaussian points varies without any criterium.

m	numeric		analytic	
	ng	M_m	nbes	M_m
0	30	-5.85e-3	150	-5.83e-3
50	40	5.97e-3 - I 1.77e-3	150	5.97e-3 - I 1.77e-3
100	50	2.39e-3 + I 4.10e-3	150	2.36e-3 + I 4.08e-3
250	60	5.22e-4 + I 1.06e-4	150	5.21e-4 + I 1.06e-4

Table 1: Comparison between numeric and analytic evaluation of the moments - $f = 50kHz$, $C = (0.3, 1)$.

m	numeric		analytic	
	ng	M_m	nbes	M_m
0	65	9.30e-3	110	9.33e-3
50	55	-8.67e-3 + I 1.77e-4	100	-8.65e-3 + I 1.74e-4
100	40	4.75e-3 - I 1.01e-3	100	4.78e-3 - I 1.01e-3
150	20	-8.76e-4 + I 1.95e-4	150	-8.79e-3 + I 1.95e-4

Table 2: Comparison between numeric and analytic evaluation of the moments - $f = 50kHz$, $C = (0.3, 0.001)$.

5 Numerical results

In order to demonstrate the accuracy and the efficiency of the proposed procedure, some numerical examples are presented. The first group of examples is aimed at showing the accuracy of the technique by comparison with some available analytical solutions. The radiating infinite cylinder with a central hole, the pulsating infinite cylinder and the scattering of a plane incident wave from an infinite cylinder are investigated. The corresponding analytical solutions are obtained in Appendix and they are compared with the results of the present procedure. The second group of

examples concerns the scattering from multiple cylinders and it is aimed at demonstrating the efficiency of the proposed procedure with respect to the conventional approach. The numerical results are obtained by discretising the boundary with at least 8 – 10 elements per wave length.

All the computations are performed on a Intel Core Duo with 3 Gb of memory running at 2.40 GHz under the Windows operating system using a home made code written in the Intel Visual Fortran Composer XE 2011 context.

5.1 Comparison with the analytical results

All the examples of this section are developed at the frequency f of 1 kHz.

The first example refers to the pulsating infinite cylinder (of radius $R = 1$) with either the pressure or the flux equal to 1 on the boundary. In both cases around 3.2 seconds are sufficient to converge to the numerical solution. The comparison in terms of amplitude of either the flux or the pressure is listed in Table 3 from which it is clear that the error is less than 0.005%.

$\bar{p}_\Gamma = 1$	Analytic	42.288
	FMBEM	42.290
$\bar{q}_\Gamma = 1$	Analytic	0.0236
	FMBEM	0.0236

Table 3: Pulsating cylinder - Comparison between analytical and FMBEM solution on the boundary.

The second example deals with a radiating (internal problem) infinite cylinder of radius $R_e = 1$ with a central cavity of radius $R_i = 0.5$ (see Fig 5).

Either the pressure is assigned unitary on both the boundaries or the flux on Γ_e and the pressure on Γ_i are imposed of unit value. The comparison is presented in Table 4. The error is always less than 0.5% and the CPU time of the numerical procedure is around 6 seconds. The third and the last example solve the scattering of an incident plane wave from an infinite cylinder. It is well known that the discretisation concerns the boundary only as the Sommerfield radiation condition is automatically satisfied by the governing integral equations. The comparison between analytical and numerical results is depicted in Figs. (6-7) with reference to the unknown value of either flux (soft scatterer) or pressure (hard scatterer) on the boundary.

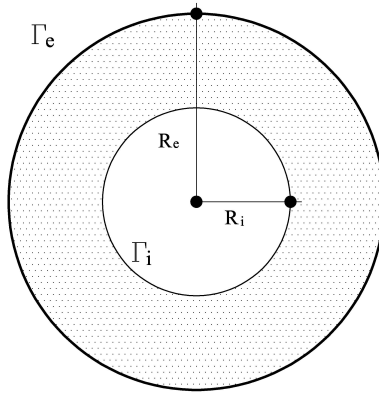


Figure 5: Radiating infinite cylinder - Internal problem

		$\bar{p}_{\Gamma_{e,i}} = 1$	$\bar{q}_{\Gamma_e} = \bar{p}_{\Gamma_i} = 1$
analytic	$ q_{\Gamma_e} $	77.79	$ p_{\Gamma_e} $ 1.431
	$ q_{\Gamma_i} $	116.2	$ q_{\Gamma_i} $ 49.83
FMBEM	$ q_{\Gamma_e} $	77.88	$ p_{\Gamma_e} $ 1.436
	$ q_{\Gamma_i} $	116.8	$ q_{\Gamma_i} $ 49.99

Table 4: Radiating cylinder with central cavity - Comparison between analytical and FMBEM solution on Γ_e and Γ_i .

5.2 Scattering from multiple cylinders

In the present section the scattering from multiple infinite soft cylinders is considered. Geometry of the problem and results are depicted in Figs. 8 and 9 separately. Each cylinder has unitary radius and it is illuminated by an incident plane wave along the horizontal axis.

The CPU time required by the FMM procedure is of the order of 1000 seconds and it is hugely inferior than the CPU time required by the conventional approach.

The CPU time for the conventional BEM approach and the proposed approach is also compared for a simple radiating infinite cylinder. In Fig 10 the CPU time is diagrammed versus the number of elements (i.e. the degrees of freedom DOFs) for increasing frequency. It is evident how the proposed approach requires a lin-

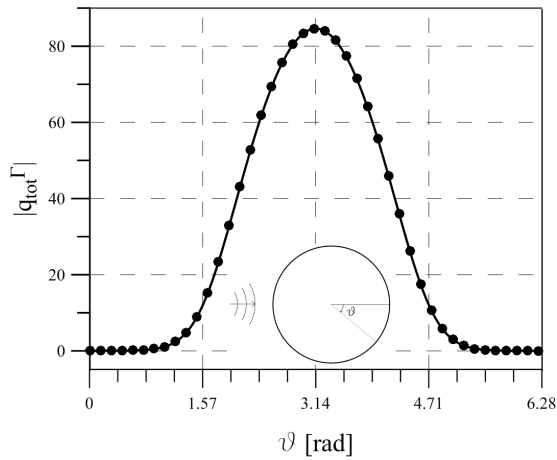


Figure 6: Scattering from a soft infinite cylinder - Comparison between the analytical results (line) and the FMBEM results (dashed circle).

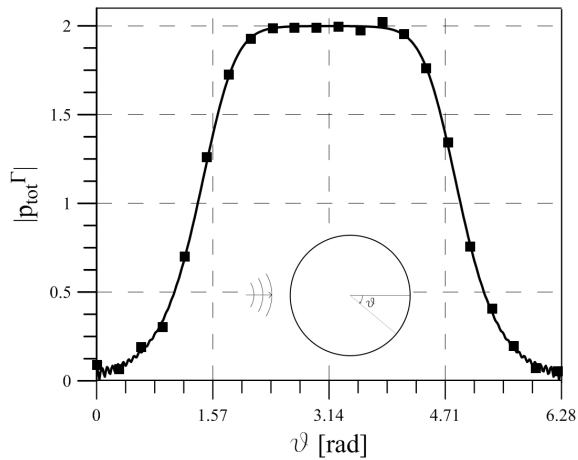


Figure 7: Scattering from a hard infinite cylinder - Comparison between the analytical results (line) and the FMBEM results (dashed circle).

early increasing CPU time with increasing DOFs; on the contrary the conventional approach requires an exponential increasing CPU time.

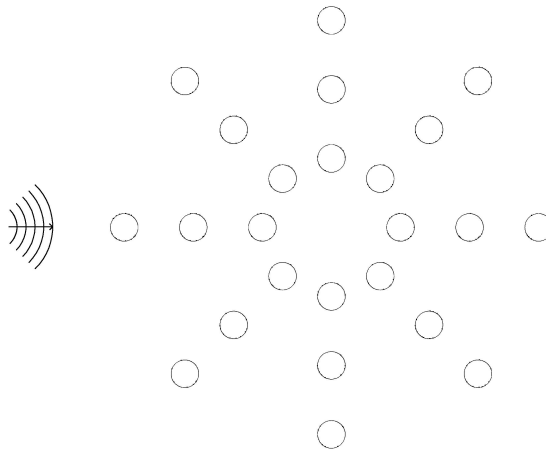


Figure 8: Geometry of the multiple scattering example.

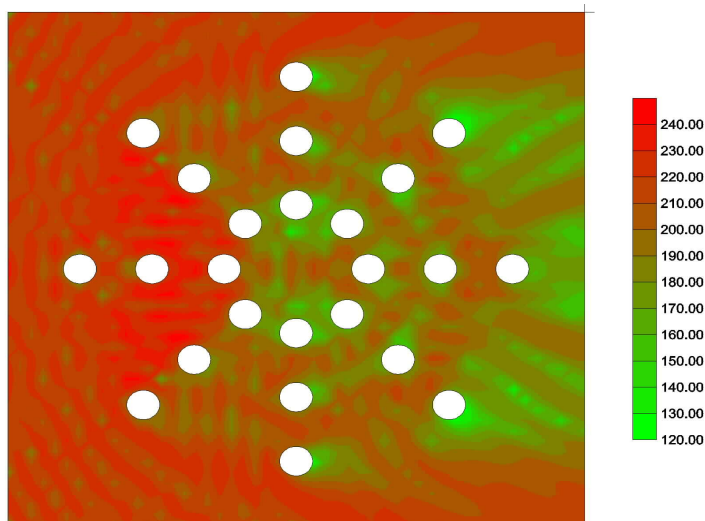


Figure 9: Multiple scattering at $f=500\text{Hz}$ - SPL in dB.

6 Conclusions

In this paper an adaptive fast multipole boundary element method for solving 2D acoustic wave problems is presented. The approach is of adaptive type, most integral terms are evaluated analytically by novel procedures, and Fortran 90 routines are developed to build the quad tree and the final system of equations. The numer-

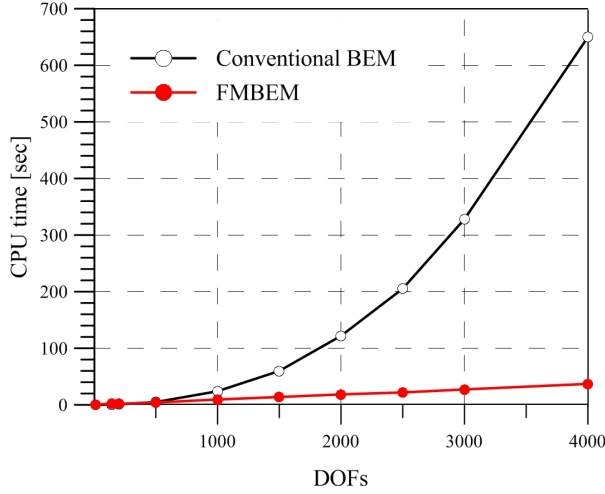


Figure 10: CPU time comparison between the conventional and the proposed approach.

ical examples show an excellent precision when compared to problems for which the analytical solution is available. The performance of the procedure is also tested in the scattering from multiple cylinder.

Appendix

The proposed FMBEM procedure is tested in the Numerical Examples section by comparing the numerical results with the analytical ones for problems for which an analytical solution is available: the radiating infinite cylinder with a central hole (internal problem), the pulsating infinite cylinder and the scattering from an infinite cylinder (both external problems). In the present appendix such analytical solutions are detailed for the sake of clearness.

The governing differential equation is the homogeneous Helmholtz equation which in polar coordinates can be written as:

$$\frac{d^2p(r)}{dr^2} + \frac{1}{r} \frac{dp(r)}{dr} + k^2p(r) = 0 \tag{24}$$

The solution corresponding to the pulsating infinite cylinder is easily obtained as:

$$p(r) = CH_0^{(2)}(kr) \tag{25}$$

where the constant can be obtained by imposing the Dirichlet/Neumann boundary

conditions on the circle with radius R , i.e.:

$$C = \begin{cases} \frac{\bar{p}}{H_0^{(2)}(kR)} & \text{if } p = \bar{p} \text{ on } \Gamma \\ -\frac{\bar{q}}{kH_1^{(2)}(kR)} & \text{if } q = \frac{\partial p}{\partial \mathbf{n}} = \bar{q} \text{ on } \Gamma \end{cases} \quad (26)$$

The solution corresponding to the radiating infinite cylinder (see Fig 5) can be written as:

$$p(r) = C_1 J_0(kr) + C_2 Y_0(kr) \quad (27)$$

where the two constants can be obtained by imposing the Dirichlet/Neumann boundary conditions on the circle and on the hole, i.e.:

$$C_1 = \begin{cases} \frac{\bar{p}_i Y_0(kR_e) - \bar{p}_e Y_0(kR_i)}{J_0(kR_i) Y_0(kR_e) - J_0(kR_e) Y_0(kR_i)} & \text{if } p = \bar{p}_e \text{ on } \Gamma_e \text{ and } p = \bar{p}_i \text{ on } \Gamma_i \\ \frac{\bar{q}_e Y_0(kR_i) + k\bar{p}_i Y_1(kR_e)}{k(J_0(kR_i) Y_1(kR_e) - J_1(kR_e) Y_0(kR_i))} & \text{if } q = \bar{q}_e \text{ on } \Gamma_e \text{ and } p = \bar{p}_i \text{ on } \Gamma_i \end{cases} \quad (28)$$

$$C_2 = \begin{cases} \frac{\bar{p}_i J_0(kR_e) - \bar{p}_e J_0(kR_i)}{J_0(kR_e) Y_0(kR_i) - J_0(kR_i) Y_0(kR_e)} & \text{if } p = \bar{p}_e \text{ on } \Gamma_e \text{ and } p = \bar{p}_i \text{ on } \Gamma_i \\ \frac{\bar{q}_e J_0(kR_i) + k\bar{p}_i J_1(kR_e)}{k(J_1(kR_e) Y_0(kR_i) - J_0(kR_i) Y_1(kR_e))} & \text{if } q = \bar{q}_e \text{ on } \Gamma_e \text{ and } p = \bar{p}_i \text{ on } \Gamma_i \end{cases} \quad (29)$$

Finally, it is simple to demonstrate that the scattering of an infinite cylinder illuminated by a plane incident wave of the type:

$$p_{inc}(r, \theta) = e^{-ikrcos(\theta - \alpha_{inc})} \quad (30)$$

where α_{inc} is the orientation of the incident wave with respect to the horizontal axis, is given by:

$$p(r) = p_{inc}(r) + p_{sc}(r) = \sum_{l=-\infty}^{\infty} \left[i^l J_l(kr) e^{il(\theta - \alpha_{inc})} + C_l H_l^{(2)}(kr) e^{il\theta} \right] \quad (31)$$

The imposition of the Dirichlet/Neumann boundary conditions on the circle provides the value of the constant C_l :

$$C_l = \begin{cases} -i^l \frac{J_l(kR)}{H_l^{(2)}(kR)} e^{-il\alpha_{inc}} & \text{if } p = 0 \text{ on } \Gamma \text{ (i.e. soft cylinder)} \\ -i^l \frac{J_l(kR)}{H_l^{(2)}(kR)} e^{-il\alpha_{inc}} & \text{if } q = 0 \text{ on } \Gamma \text{ (i.e. hard cylinder)} \end{cases} \quad (32)$$

References

- Abramowitz, M.; Stegun, I.A.** (1964): *Handbook of Mathematical Functions*. M. Abramowitz and I. Stegun (eds), New York.
- Aliabadi, M. H.** (2002): *The Boundary Element Method Volume 2: Applications in Solids and Structures*. Wiley, Chichester, West Sussex.
- Bapat, M.S.; Liu, Y.J.** (2010): A new adaptive algorithm for the Fast Multipole Boundary Element Method. *CMES: Computer Modeling in Engineering & Sciences*, vol. 58, no. 2, pp. 161-183.
- Brancati, A.; Aliabadi, M. H.; Mallardo, V.** (2012): A BEM sensitivity formulation for three-dimensional active noise control. *Int. J. Numer. Meth. Engng.*, vol. 90, pp. 1183-1206.
- Brunner, D.; Junge, M.; Rapp, P.; Bebendorf, M.; Gaul, L.** (2010): Comparison of the Fast Multipole Method with Hierarchical Matrices for the Helmholtz-BEM. *CMES: Computer Modeling in Engineering & Sciences*, vol. 58, no. 2, pp. 131-158.
- Chen, J. T.; Chen, K. H.** (2004): Applications of the dual integral formulation in conjunction with fast multipole method in large-scale problems for 2D exterior acoustics. *Eng. An. Bound. Elem.*, vol. 28, pp. 685-709.
- Li, S.; Huang, Q.** (2011): A new fast multipole boundary element method for two dimensional acoustic problems. *Comput. Methods Appl. Mech. Engrg.*, vol. 200, pp. 1333-1340.
- Liu, Y. J.; Nishimura, N.** (2006): The fast multipole boundary element method for potential problems: A tutorial. *Eng. An. Bound. Elem.*, vol. 30, pp. 371-381.
- Mallardo, V.; Aliabadi, M. H.** (2011): A novel DRBEM application for nonlinear wave propagation. *Int. J. Numer. Meth. Biomed. Engng.*, vol. 27, pp. 238-250.
- Mallardo, V.; Aliabadi, M. H.; Brancati, A.; Marant, V.** (2011): An accelerated BEM for simulation of noise control in the aircraft cabin. *Aerospace Science and Technology*, doi:10.1016/j.ast.2011.10.001.
- Nishimura, N.** (2000): Fast multipole accelerated boundary integral equation methods. *Appl. Mech. Rev.*, vol. 55, no. 4, pp. 299-324.
- Ramesh, P. S.; Lean, M. H.** (1991): Accurate integration of singular kernels in boundary integral formulations for Helmholtz equation. *Int. J. Numer. Methods Eng.*, vol. 31, pp. 1055-1068.
- Rokhlin, V.** (1983): Rapid solution of integral equations of classical potential theory, *J. Comput. Phys.*, vol. 60, pp. 187-207.
- Rokhlin, V.** (1990): Rapid solution of integral equations of scattering theory in two

dimensions, *J. Comput. Phys.*, vol. 86, pp. 414-439.

Saad, Y.; Schultz, M. (1986): GMRES: A generalized minimal residual algorithm for solving non-symmetric linear systems. *SIAM J. Sci. Stat. Comput.*, vol. 7, pp. 856-869.

Shen, L.; Liu, Y. J. (2007): An adaptive fast multipole boundary element method for three-dimensional acoustic wave problems based on the Burton-Miller formulation. *Comput. Mech.*, vol. 40, pp. 461-472.

Singh, K. M.; Tanaka, M. (2000): Analytical integration of weakly singular integrals in boundary element analysis of Helmholtz and advection-diffusion equations. *Comput. Methods Appl. Mech. Engrg.*, vol. 189, pp. 625-640.

Wang, P.B.; Yao, Z.H.; Lei, T. (2006): Analysis of Solids with Numerous Microcracks Using the Fast Multipole DBEM. *CMC: Computers, Materials & Continua*, vol. 3, no. 2, pp. 65-75.

Watson, G. (1966): *A treatise on the theory of Bessel functions*. Cambridge University Press.

Wrobel, L. C. (2002): *The Boundary Element Method Volume 1: Applications in Thermo-Fluids and Acoustics*. Wiley, Chichester, West Sussex.